

On the Impulse Response of a Coupled-Mode System

C. W. BARNES, SENIOR MEMBER, IEEE

Abstract—The impulse response is derived for a simple coupled-mode system in which two modes of propagation are passively coupled. It is found that if one mode is driven with an impulse, the response of the other mode consists of a sharply defined RF pulse, of constant maximum amplitude, whose length increases linearly with both time and distance of propagation. The energy of the coupled pulse is found to approach an equilibrium value as the time (or length) of interaction increases without limit.

I. INTRODUCTION

WE CONSIDER HERE a linear, uniform, lossless, passive, wave transmission system of infinite length in which two modes of propagation, with group velocities in the same direction, are weakly coupled together. The type of coupling that occurs under these conditions is called "passive mode coupling,"¹ or "co-flow hermitian coupling,"² and is characterized by the frequency-domain coupled-mode equations,^{1,2}

$$\frac{\partial \hat{a}_1(z, \omega)}{\partial z} = -i\beta_1 \hat{a}_1(z, \omega) - i\kappa \hat{a}_2(z, \omega) \quad (1)$$

$$\frac{\partial \hat{a}_2(z, \omega)}{\partial z} = -i\kappa^* \hat{a}_1(z, \omega) - i\beta_2 \hat{a}_2(z, \omega) \quad (2)$$

where $\hat{a}_1(z, \omega)$ and $\hat{a}_2(z, \omega)$ are the frequency-domain amplitudes of the two modes, β_1 and β_2 are the (uncoupled) propagation constants of the two modes, and κ is the complex coupling coefficient between the two modes. The behavior of this type of coupled-mode system, for an input that varies sinusoidally with time, consists of the familiar periodic interchange of power between the two modes.^{1,2,3} It is the purpose of this paper to point out the rather curious response that this coupled system exhibits when the input to one of the modes is an impulse (or delta function) in time. In particular, we shall examine the response of Mode 2 when Mode 1 is driven with an impulse.

For weak coupling, the nature of the interaction will depend only upon the characteristics of the system at frequencies in the neighborhood of the frequency at which the two modes have equal phase velocities. Thus,

Manuscript received January 18, 1965; revised March 15, 1965. This work was supported by the Air Force Systems Command, Research and Technology Div., Rome Air Development Center, Griffiss AFB, New York, N. Y.

The author is with Stanford Research Institute, Menlo Park, Calif.

¹ Louisell, W. H., *Coupled Mode and Parametric Electronics*. New York: Wiley, 1960, ch. 1, pt. II.

² Barnes, C. W., "Conservative coupling between modes of propagation—a tabular summary," *Proc. IEEE*, vol. 52, Jan 1964, pp. 64-73.

³ Pierce, J. R., "Coupling of modes of propagation," *J. Appl. Phys.*, vol. 25, Feb 1954, pp. 179-183.

we shall be able to derive some rather general results without having to make any severely restrictive assumptions about the nature of the modes.

II. ANALYSIS

We consider two modes of propagation whose uncoupled $\omega-\beta$ characteristics intersect as shown in Fig. 1. If the coupling between the two modes is weak, then the only significant interaction occurs at frequencies in the neighborhood of ω_0 , the frequency at which the two uncoupled modes have equal phase velocities. We shall assume that in the neighborhood of ω_0 , the uncoupled $\omega-\beta$ characteristics of the two modes can be approximated by the straight lines described by

$$\beta_1 = \beta_0 + (\omega - \omega_0)/v_1 \quad (3)$$

and

$$\beta_2 = \beta_0 + (\omega - \omega_0)/v_2 \quad (4)$$

where v_1 and v_2 are the group velocities⁴ of the two modes at frequency ω_0 . We further assume that the coupling coefficient κ , which we write in the phasor form,

$$\hat{\kappa} = \kappa e^{i\phi} \quad (5)$$

is a sufficiently slowly varying function of frequency so that, for the weak coupling case, we can approximate it in the neighborhood of ω_0 by a constant.

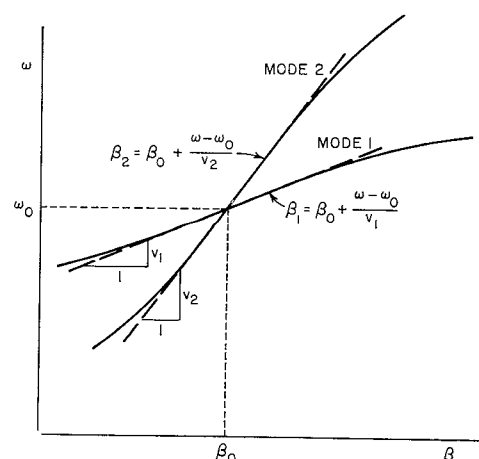


Fig. 1. $\omega-\beta$ Characteristics of the uncoupled modes.

⁴ In order to be explicit, we shall assume throughout the analysis that $v_2 > v_1$. This does not restrict the generality of the results. The behavior of the system for the alternate case is, *mutatis mutandis*, essentially the same.

The solution of (1) and (2) for the amplitude of Mode 2 in terms of the boundary conditions at the input (i.e., at $z=0$) is^{1,2}

$$\begin{aligned}\hat{a}_2(z, \omega) = & \left\{ \hat{a}_1(0, \omega) \left[-i \frac{\kappa^*}{\xi} \sin \xi z \right] \right. \\ & + \hat{a}_2(0, \omega) \left[\cos \xi z + i \frac{\Delta\beta}{2\xi} \sin \xi z \right] \left. \right\} \\ & \cdot \exp \left[-i \left(\frac{\beta_1 + \beta_2}{2} \right) z \right] \quad (6)\end{aligned}$$

where

$$\Delta\beta = \beta_1 - \beta_2 \quad (7)$$

and

$$\xi = [\kappa^2 + (\Delta\beta/2)^2]^{1/2}. \quad (8)$$

The time-domain mode amplitudes are related to the frequency-domain mode amplitudes by the Fourier transform relation⁵

$$a(z, t) = \frac{1}{2\pi} \int_0^\infty \hat{a}(z, \omega) e^{i\omega t} d\omega + \text{c.c.} \quad (9)$$

where c.c. indicates the complex conjugate.

We now consider the case where the boundary conditions at $z=0$ are given by

$$a_1(0, t) = a_0 \delta(t) \quad (10)$$

and

$$a_2(0, t) = 0 \quad (11)$$

or

$$\hat{a}_1(0, \omega) = a_0 \quad (12)$$

and

$$\hat{a}_2(0, \omega) = 0 \quad (13)$$

where $\delta(t)$ is the unit impulse and a_0 is a real constant.

If we now substitute into (6) the boundary conditions, given by (12) and (13), and the expressions for β_1 and β_2 , given by (3) and (4), we find that the frequency-domain amplitude of Mode 2 can be written in the form

$$\begin{aligned}\hat{a}_2(z, \omega) = & -i A_2(z, \omega - \omega_0) \exp \left\{ -i \left[\beta_0 z + \left(\frac{\omega - \omega_0}{2} \right) \right. \right. \\ & \left. \left. \cdot \left(\frac{1}{v_1} + \frac{1}{v_2} \right) z + \phi \right] \right\} \quad (14)\end{aligned}$$

⁵ By writing the Fourier transform relation in the form given by (9), rather than the more familiar double-sided form, we avoid the necessity of explicitly considering the coupled-mode interactions at negative frequencies; the negative frequencies are taken care of automatically by the addition of the complex conjugate term.

where

$$A_2(z, \omega) = a_0 \left(1 + \frac{\omega^2}{\omega_1^2} \right)^{-1/2} \sin \left[\kappa z \left(1 + \frac{\omega^2}{\omega_1^2} \right)^{1/2} \right] \quad (15)$$

and

$$\omega_1 = 2\kappa \left(\frac{1}{v_1} - \frac{1}{v_2} \right)^{-1}. \quad (16)$$

Note that the parameter ω_1 , which is directly proportional to the magnitude of the coupling coefficient κ , is a measure of the angular bandwidth of the coupled-mode interaction. In terms of ω_1 , the criterion for the weak-coupling (or narrow-band) case is, therefore,

$$\omega_1 \ll \omega_0. \quad (17)$$

The time-domain amplitude of Mode 2 is now obtained by substituting (14) into (9). The evaluation of the integral in (9) is greatly simplified if we note that for the weak coupling case (where $\omega_1 \ll \omega_0$), we can extend the lower limit of the integral to $-\infty$ without incurring significant error; upon doing this, we find that the time domain amplitude is given by

$$a_2(z, t) = F(z, t) \sin (\omega_0 t - \beta_0 z - \phi) \quad (18)$$

where

$$F(z, t) = a_0 \omega_1 J_0 \left\{ \omega_1 \left[\left(t - \frac{z}{v_2} \right) \left(\frac{z}{v_1} - t \right) \right]^{1/2} \right\} \quad (19)$$

for

$$(z/v_2) < t < (z/v_1),$$

and

$$F(z, t) = 0 \quad (20)$$

for

$$t < (z/v_2) \quad \text{or} \quad t > (z/v_1).$$

Thus, we see that the response of Mode 2 to an impulse input on Mode 1 consists of a wave of the form $\sin (\omega_0 t - \beta_0 z)$ that is modulated in amplitude by a single pulse. A sketch of a typical form of the pulse envelope, as a function of z , is shown in Fig. 2. Note that the pulse envelope has a sharp leading edge that travels with velocity v_2 and a sharp trailing edge that travels with velocity v_1 . The maximum amplitude of the pulse envelope is independent of both z and t , and the pulse envelope length, measured along the z axis, increases linearly with time. The pulse envelope length, measured along the t axis, increases the linearly with z .

In Fig. 3 we show a normalized time sequence for the pulse envelope for the special case where $v_2 = 2v_1$. In these plots, the point where $\kappa z = \pi/2$ is marked for reference since this is the point at which total power trans-

fer to Mode 2 would have occurred if the input to Mode 1 had been a sinusoid at frequency ω_0 .

It is also interesting to consider the total energy carried by the pulse on Mode 2. The spectral energy density in Mode 2 is given by

$$u(z, \omega) = \frac{\hat{a}_2(z, \omega)\hat{a}_2^*(z, \omega)}{2\pi W(\omega)} \quad (21)$$

where $W(\omega)$ is an appropriate immittance function for Mode 2. The total energy carried past a given point z is, therefore,

$$U(z) = \frac{1}{2\pi} \int_0^\infty \frac{\hat{a}_2(z, \omega)\hat{a}_2^*(z, \omega)}{W(\omega)} d\omega. \quad (22)$$

If the immittance function $W(\omega)$ is a slowly varying function of ω in the neighborhood of ω_0 , then for the weak coupling case we can approximate $W(\omega)$ in the neighborhood of ω_0 by

$$W(\omega) \approx W(\omega_0) = W_0. \quad (23)$$

Also, for the weak coupling case, we can extend the lower limit of the integral in (22) to $-\infty$ without incurring significant error. Thus, upon substituting (23) and (14) into (22) and extending the lower limit of integration, we find that

$$U(z) = \frac{1}{2\pi W_0} \int_{-\infty}^\infty [A_2(z, \omega - \omega_0)]^2 d\omega \quad (24)$$

or

$$U(z) = \frac{\omega_1 a_0^2}{2\pi W_0} \int_{-\infty}^\infty (1 + s^2)^{-1} \sin^2 [\kappa z(1 + s^2)^{1/2}] ds \quad (25)$$

where

$$s = \frac{\omega - \omega_0}{\omega_1}. \quad (26)$$

If we make the change of variables $s = \sinh x$ in (25), differentiate with respect to z , recognize a familiar Bessel function identity and then integrate with respect to z we find that the pulse energy can be expressed in the form

$$U(z) = \frac{a_0^2 \omega_1}{4W_0} \int_0^{2\kappa z} J_0(x) dx. \quad (27)$$

Fortunately, the integral in (27) has been tabulated.⁶ In Fig. 4 we have plotted the normalized pulse energy as a function of κz . Note that as κz increases, the pulse energy goes through a sequence of maxima and minima

⁶ Abramowitz, M., and I. A. Stegun, *Handbook of Mathematical Functions*, NBS Appl. Math. Ser., U. S. Government Printing Office, 1964, vol 55.

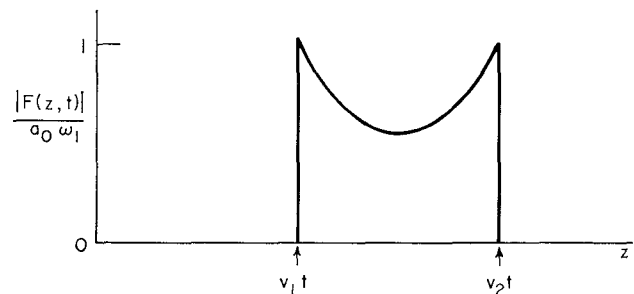


Fig. 2. Typical form of pulse envelope on Mode 2 in response to an impulse input of magnitude a_0 on Mode 1.

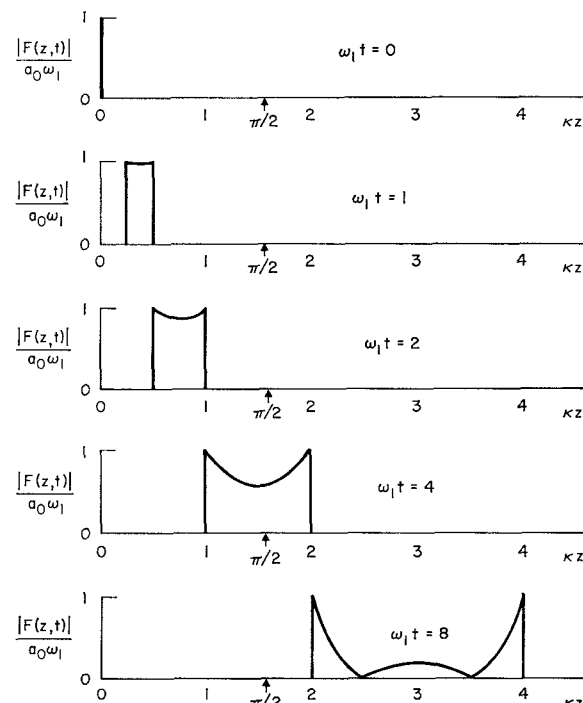


Fig. 3. A time sequence of pulse envelopes on Mode 2 for the case where $v_2 = 2v_1$.

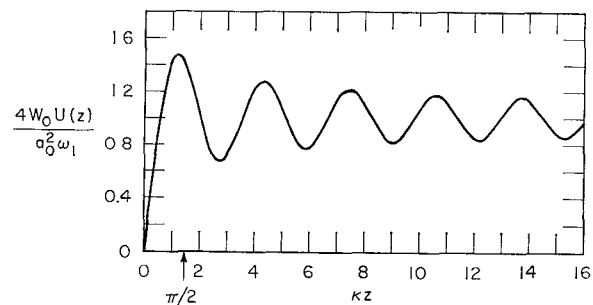


Fig. 4. Total energy in the pulse on Mode 2 for an impulse input of magnitude a_0 on Mode 1.

and ultimately, for $\kappa z \gg 1$, approaches an equilibrium value. That is,

$$U(z) \rightarrow \frac{a_0^2 \omega_1}{4W_0} \quad (28)$$

as $z \rightarrow \infty$. The first maximum, where the pulse energy overshoots the equilibrium value by almost 50 per cent, occurs at the smallest value of κz for which

$$J_0(2\kappa z) = 0; \quad (29)$$

that is, at

$$\kappa z = 1.202. \quad (30)$$

The position of the first maximum could be used as a basis for measurement of the coupling coefficient in a coupled-mode system.

Thus, as the pulse on Mode 2 propagates along the transmission system, the pulse length grows without bound and the shape of the pulse envelope continues to change, but the energy of the pulse approaches an equilibrium value that is directly proportional to the magnitude of the coupling coefficient.

III. COMMENTS

Coupled-mode systems are customarily characterized by their frequency-domain response. We have presented here a derivation of the time-domain response of an important class of coupled-mode systems; we hope that this derivation will provide new insights into the behavior of these systems.

The principal assumptions that we have made are 1) that the coupling coefficient between modes is independent of frequency, and 2) that the $\omega - \beta$ characteristics of the two modes are straight lines. Note that the assumption of a linear $\omega - \beta$ characteristic is not the same as an assumption of zero dispersion. It is clear from (14) and (15) that for weak coupling, most of the energy transfer between modes occurs in the frequency range $\omega_0 - \omega_1$ to $\omega_0 + \omega_1$. Thus, if the $\omega - \beta$ characteristics are straight *in this frequency range*, and the coupling coefficient is constant *in this frequency range*, then the results that we have derived here should be approximately correct. If the $\omega - \beta$ characteristics deviate from linearity outside of the frequency range $\omega_0 - \omega_1$ to $\omega_0 + \omega_1$, the resulting effect would probably be a rounding of the sharp edges of the pulse on Mode 2.

A Precise and Sensitive X-Band Reflecto“meter” Providing Automatic Full-Band Display of Reflection Coefficient

F. C. DE RONDE

Abstract—A simple waveguide system has been made for the instantaneous measurement of the magnitude of the reflection coefficient as a function of frequency for the 8.2–12.4 Gc band.

Reflection coefficients in the range 1 to 0.001 can be measured on linear scales; above 0.01 the error is less than ± 3 per cent, below 0.01 it is estimated to be in the order of ± 5 per cent.

By using a long line between the unknown impedance and the two wall-current detectors, which act as measuring probes, an audio-frequency voltage has been obtained which is linearly proportional to the amplitude of the unknown reflection coefficient.

A third wall-current detector is used as a leveler.

The principle is quite simple and can easily be applied for other frequencies or transmission lines.

Manuscript received November 16, 1964; revised March 19, 1965.
The author is with Philips Research Laboratories, N.V. Philips' Gloeilampenfabrieken, Eindhoven, The Netherlands.

I. INTRODUCTION

REFLECTO“METERS” using directional couplers and a ratiometer are commonly used for swept-frequency display. Although they work much faster than standing-wave indicators their accuracy is considerably lower. A great improvement over the usual method of two couplers together with broadband detectors can be obtained if one directional coupler with built-in wall-current detectors [1], [2] is used. However, the finite directivity of the directional coupler and its variation with frequency limits the accuracy especially at very low values of the reflection coefficient, while reflection of the coupler limits it at very high values.